Proceedings of the Estonian Academy of Sciences,
2016, **65**, 3, 284–296
doi: 10.3176/proc.2016.3.05
Available online at www.eap.ee/proceedings

ENGINEERING

Assemblage of turbulent jet flows through static particulate media

Peep Lauk[a*], Josep Hueso Rebassa[b], Aleksander Kartushinsky[c], Sergei Tisler[c], Toivo Tähemaa[d], and Andrei Polonsky[e]

[a] Department of Aircraft Engineering, Estonian Aviation Academy, Lennu 40, Reola, Ülenurme, 61707 Tartu County, Estonia
[b] ETSEIAT, Polytechnic University of Catalonia, Colom Street 11, 08222 Terrassa, Spain
[c] Chair of Fluid Mechanics, Department of Mechanics, Faculty of Civil Engineering, Tallinn University of Technology, Ehitajate tee 5, 19086 Tallinn, Estonia
[d] Chair of Product Development, Department of Mechanical and Industrial Engineering, Faculty of Mechanical Engineering, Tallinn University of Technology, Ehitajate tee 5, 19086 Tallinn, Estonia
[e] Nordisc Sikkerhet, Lommedalsveien 182, 1353 Bærums Verk, Norway

Received 27 May 2015, revised 20 November 2015, accepted 23 November 2015, available online 3 August 2016

Abstract. The work consists in numerical modelling of two-phase flow in porous media. The performance of a vertical cylinder pellets dryer with four lateral jets discharging air to a motionless particulate medium was modelled. The aim was to better understand the mechanism of heat exchange and the effect of different parameters on the fluid going through a particulate medium. The flow was considered non-isothermal and turbulent. The cases were first calculated for a single phase (isothermal and non-isothermal) and then for two phases with changing the particles volume fraction and size. The Boussinesq approach was used to take into account the effect of temperature on the gas velocity, and the k–ε model was applied for the closure of momentum equations. The solution algorithm was built using a scheme of finite differences with the tri-diagonal matrix algorithm. The results show how different variables, such as axial velocity or temperature of lateral jets flow, start with high values in the inlets and merge and collapse further downstream while the flow goes through the medium. The axial velocity drops from the jets up to the end of the system. This drop is higher for larger particles volume fractions. The radial velocity tends to increase from a null value faster for larger particles volume fractions. As the drag increases, the temperature drops faster for larger particles volume fractions and for bigger particles, which can be explained by the higher energy transfer between the flow and the particles.

Key words: assemblage of jets, multi-phase flow, particulate media, non-isothermal turbulent flow, RANS modelling, TDMA method, pellet dryer.

1. INTRODUCTION

During the last few decades, the drying technology has been improved because of the need of more efficient industrial processes, in order to reduce the power consumption and the time spent, and also to reach lower levels of humidity on the particles. As the air has to be discharged to the system using jets, the investigation of the physical processes involved in the turbulent jets has also improved significantly, from the single isolated jet to systems of multiple jets that have a strong interaction.

1.1. Industrial dryers

Traditionally, grain drying takes place in separate drying equipment outside storage silos. Typically, it involves burning high volumes of fuel to heat the drying air. Early on-farm drying was done in walled silos using vertical motion of air forced under fan pressure into an air chamber beneath a perforated floor. Heated air is forced

* Corresponding author, peep.lauk@eava.ee

upward through a thick layer of grain. Two main technologies of vertical flow dryers are the 'layer-in-silo grain dryer' and the 'batch-in-silo grain dryer'. The former was developed in the USA in the late 1940s, and it required grain levellers to add uniform layers of grain. The latter was developed in order to improve the performance and to alleviate the over-drying problem [1].

Oklahoma State University demonstrated in the 1960s that moving the same volume of air horizontally from ducts on one side of a silo to the opposite side requires less power and static pressure compared to the same airflow rates moved vertically [2,3]. Then a new technology called 'in-silo cross-flow grain aeration and drying technology' emerged. It involved a high air-flow delivery with low static pressure and low fan power, which was highly beneficial to worldwide grain systems for the in-silo grain drying. It can allow higher airflows for lower cost. The goal was to operate the airflow system continuously from relatively low fill levels until the silo is full [4,5]. The 'alternative cross-flow in-silo dryer configuration' is the latest achievement in the drying technology; the exhaust vents comprise adjustable air valves and so the air volume can be proportionally controlled at each level of the dryer. The full height centred vertical aerator tube distributes drying air radially, directly to the outer perforated wall plenums. As air 'fans out' from the vertical aerator pipe, the air velocity gradually decreases, providing an increased cooling or drying time in the outer grain [1].

1.2. Theoretical background

Focusing on the background of the fluid dynamics development and research, several analytical, experimental, and computational studies have been made over the past decades dealing with the flow structure and characteristics of laminar and turbulent round and symmetrical jets, as well as multiple jet systems and the flows through particles, which can be considered similar to a flow through porous media [6–8].

1.2.1. Single round symmetrical jet

The classical study by Abramovich [9] and other developments on this topic make this kind of jet one of the most well-known problems in fluid dynamics. However, because of the computational limitations in the past, all previous studies and models have been made using some simplifications of the structure of the jet, the behaviour of the particulate phase, or the interactions of the phases. In order to better understand the given process, Abramovich [9] used Prandtl's mixing-length theory to take into account the feedback of the particles on the turbulent structure and predicted attenuation of turbulence by the particles. This effect was not confirmed experimentally or numerically until almost two decades later and for fine particles only [10,11]. Experimental investigations of two-phase jets were performed by some researchers who investigated how the fluid velocity and turbulent kinetic energy structures are affected by the presence of droplets [12] or solid particles [13].

With the development of electronics and computation, more complicated studies related to the turbulent particulate jets have been made using the turbulent boundary layer approach [14,15]. In the last ten years, numerical studies have examined several aspects of the flow and structure of turbulent jets. The modelling of an isothermal turbulent round jet carrying small and large particles was accomplished using a large-eddy simulation approach coupled with the Lagrangian method for the modelling of particles in the particulate phase [16].

A full numerical simulation using the Reynolds Averaged Navier–Stokes (RANS) equations is the subject of the current investigation. The two-phase turbulent boundary layer approximation is applied within the RANS approach, which is reasonably relevant and usually applied for modelling the behaviour of two-phase round jets.

The system of equations for the mass and momentum conservation equations and the turbulence closure equations (the extended k–ε model) were derived and solved using a finite difference scheme [17]. The two-way coupling model, first presented in [18], was used along with the particulate feedback onto the average distribution of the carrier phase via the forces acting on the particles. The coefficient of the turbulent diffusion of particles was used to close the mass conservation equation for the particulate phase. Similarly, the introduction of the particle turbulent viscosity coefficient was used as a closure equation for the momentum equation of the particulate phase, called 'the extended k–ε model for particle–turbulence interactions' [17,19].

1.2.2. Multiple jets

Since 1944 some experiments have been made in order to understand how different jets interact. Two important phenomena were found in those experiments: the amalgamation of jets after a certain distance to create a single jet and the deflection of side jets toward the centre of the system [20–22].

The merging is due to jet spreading rather than the deflection of the jets towards the centre and is related to the confined arrangement of multiple jets. A system of multiple jet burners with a central fuel jet surrounded by a ring of either four or six air jets was performed. It was found that the jets from the outer nozzles curve towards the centreline of the array while merging with each other and the centre jet. This overall contraction is the result of the entrainment action of each jet, which draws in fluid from the surroundings, and thus produces suction on its neighbours [22].

The experimental data and numerical simulations obtained for the assemblage of jets show three regions. An initial region with a constant jet velocity and low velocities between the jets is located near the nozzle plate. The next region is dominated by strong jet-to-jet interactions and a fall in the jet velocity. In the final stages, individual jets can no longer be observed, and the turbulence decays [23,24].

1.3. Aim of the work

The aim of this work was first to solve a complex problem involving four jets with a relatively low separation between them, discharging air to the system and with an inlet temperature that makes the problem non-isothermal. To solve the complicated flow resulting from the interaction between the flows of the jets and between the flows and the boundaries is the main goal to reach. In addition, as a second step, the system was filled with particles, making the problem even more complicated, resulting in a turbulent two-phase (gas–solids) fluid dynamics problem related to the cross-flow grain dryer, with the jets discharging air to a particulate medium with a specificity of the static particles. As it is a model of a pellet dryer, it has to evaporate the moisture of the wet particles and decrease their humidity, so this is a non-isothermal problem.

Thus, the goal was to study how the flow evolves through the multiple jet system, first in a single-phase system and then in a particulate medium, and to investigate the influence of particles on the jet system and their effect on the flow in terms of velocity, temperature, turbulence, and particles diffusion.

The numerical results of this work could be a reference for future studies and designs of cross-flow grain dryers. The future steps will be to calculate the variation of the humidity of the particles, but the current work is focused on the flow field without considering this effect.

2. NUMERICAL MODEL

The cross-flow grain dryer used consists of a large cylinder with a circular pipe centred on it from where the air moves inside a toroidal particle hopper. The pipe has four jets, which are responsible for discharging air to the particulate medium. To be precise, there are three and a half jets because the first jet is only a half and it is placed on the top of the cylinder (as shown in Fig. 1). After travelling through the particulate medium, made of wooden spherical particles with a physical density of 650 kg/m^3, the air leaves the system.

As the numerical model was built for solving the two-dimensional case, only a slice of the toroidal hopper will be taken into account due to the symmetry. The

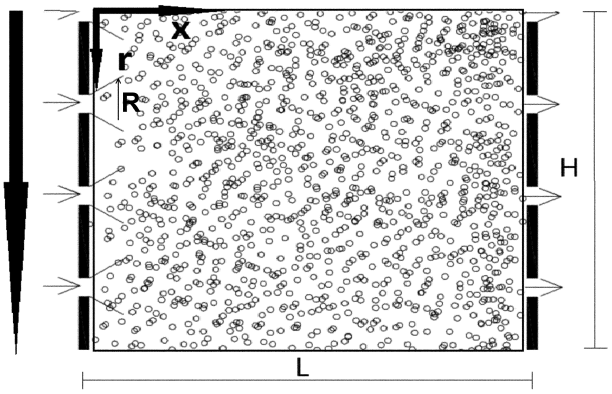

Fig. 1. Scheme of the particles dryer. R – jet radius, L – hopper width, x – axial direction of the jets, r – radial coordinate.

dimensions of the dryer are defined in terms of the radius of each jet R, where $R = 51$ mm. The width L of the hopper is $320R$, the height H is $20R$. The distance between the jets is $2.25R$.

The coordinate system used for the calculations is a polar system centred on the jets, so the x direction is the axial direction of the jets, and the r is the radial coordinate. As it is the two-dimensional case, the r coordinate corresponds to the y coordinate of the Cartesian system.

2.1. Governing equations

As the gas and particle velocities are much lower than the velocity of sound, the gas flow was considered to be incompressible. The equations used to solve this system are RANS equations, which are volume-averaged in two dimensions using the polar coordinates [17]. This is a multiphase problem that involves the gas flow and solid particles; however, as solid particles have no motion, the equations solved are only the ones covering the gas flow, but including interactions with the particles, such as the forces due to the difference of velocities between phases or the energy exchange.

The first equation is a continuity equation:

$$\frac{\partial u}{\partial x} + \frac{\partial (rv)}{r\partial r} = 0, \tag{1}$$

where x and r are the axial and radial coordinates; u and v are the axial and radial velocity components of the gaseous phase.

The next equation is an equation of momentum conservation in the axial direction:

$$\rho u \frac{\partial u}{\partial x} + \rho v \frac{\partial u}{\partial r} = \frac{\partial}{r\partial r} r\nu_t \frac{\partial u}{\partial r} - \frac{\alpha (u - u_s)}{\tau}, \tag{2}$$

where u_s and v_s are the axial and the radial velocity of the particulate phase, respectively; v and v_t are the coefficient of the laminar and of the turbulent viscosity, respectively; τ is the characteristic time of the particles and it is connected with the drag force produced by the particulate phase:

$$\tau = \left[\acute{C}_D \left(\frac{18\rho v}{\rho_p d^2} \right) \right]^{-1}, \tag{3}$$

where ρ and ρ_p are the physical densities of gas and particles, respectively; d is the particle diameter; $\acute{C}_D$ is a correction factor for the non-Stokesian drag on the particles; and Re_s is the Reynolds number of the particles [25]:

$$\acute{C}_D = 1 + 0.15 Re_s^{0.687}, \tag{4}$$

$$Re_s = \frac{d\sqrt{(u-u_s)^2 + (v-v_s)^2}}{v}. \tag{5}$$

The mass concentration of the particulate phase α is determined as follows:

$$\alpha = \beta \frac{\rho_p}{\rho}, \tag{6}$$

where β is the volume fraction of the particulate phase.

The transport of momentum in the radial direction is not needed since the pressure is not going to be solved. It seems to be a good approximation for neglecting the effect of the pressure gradient as the difference of the pressure inside and outside the jet is minimal. The boundary layer approximation was assumed, and as a result the diffusive terms were neglected for the axial direction.

The radial velocity of the particulate jet was obtained from the combination of equations of conservation of momentum in the axial direction and the continuity equation. It is given by the integral [14,26]:

$$v = -\frac{u}{r} \int_0^r \frac{r dr}{u^2} \left[\frac{\partial}{r \partial r} r v_t \frac{\partial u}{\partial r} - \frac{\alpha (u - u_s)}{\tau} \right]. \tag{7}$$

The turbulent kinetic energy and the rate of dissipation were built using the k–ε model, where k and ε are the kinetic turbulent energy and its dissipation rate, respectively:

$$u \frac{\partial k}{\partial x} + v \frac{\partial k}{\partial r} = \frac{\partial}{\partial x} \left(\frac{v_t}{\sigma_k} \frac{\partial k}{\partial x} \right) + \frac{\partial}{r \partial r} r \left(\frac{v_t}{\sigma_k} \frac{\partial k}{\partial r} \right) + P_k + P_s - \varepsilon, \tag{8}$$

$$u \frac{\partial \varepsilon}{\partial x} + v \frac{\partial \varepsilon}{\partial r} = \frac{\partial}{\partial x} \left(\frac{v_t}{\sigma_\varepsilon} \frac{\partial \varepsilon}{\partial x} \right) + \frac{\partial}{r \partial r} r \left(\frac{v_t}{\sigma_\varepsilon} \frac{\partial \varepsilon}{\partial r} \right) + \frac{\varepsilon}{k} [C_{\varepsilon 1} (P_k + P_s) - C_{\varepsilon 2} \varepsilon], \tag{9}$$

$$P_k = v_t \left\{ 2 \left[\left(\frac{\partial u}{\partial x} \right)^2 + \left(\frac{\partial v}{\partial r} \right)^2 \right] + \left[\frac{\partial u}{\partial r} + \frac{\partial (rv)}{r \partial r} \right]^2 \right\}, \tag{10}$$

$$P_s = \frac{\alpha [(u-u_s)^2 + (v-v_s)^2]}{\tau}, \tag{11}$$

$$v_t = C_\mu \left(\frac{k^2}{\varepsilon} \right). \tag{12}$$

Here P_k is the turbulent production by the velocity gradients and P_s is the turbulent production by the average velocity slip between the gas and the particles. The turbulent viscosity v_t (Eq. (12)) is obtained by the closure equations (Eqs (8) and (9)), with the typical values for the k–ε model, which are $\sigma_k = 1$, $\sigma_\varepsilon = 1.3$, $C_{\varepsilon 1} = 1.44$, $C_{\varepsilon 2} = 1.92$, $C_\mu = 0.09$ [18].

The equation of energy balance is as follows:

$$\rho u \frac{\partial T_f}{\partial x} + \rho v \frac{\partial T_f}{\partial r} = \frac{\partial}{r \partial r} \frac{r v_t}{Pr} \frac{\partial T_f}{\partial r} - \rho \alpha \frac{(T_f - T_s)}{\tau}, \tag{13}$$

where T_f and T_s are the temperatures of the gas and the particles, respectively. The Prandlt number Pr is taken as 0.8.

The particles were placed all together and they will have restrictions of their motion. This is a good approximation to impose the zero velocity for the particles and simplify the equations:

$$u_s = 0, \tag{14}$$

$$v_s = 0. \tag{15}$$

2.2. Boundary conditions

The considered system has various boundary conditions: the inlet conditions on the jets, the conditions on the top and the bottom of the system, and finally the outlet conditions. The variables of the flow are expressed in a non-dimensional form following Eqs (16)–(18), where pipe refers to the inlet of the system before going through the jets:

$$U = \frac{u}{U_{\text{pipe}}}, \tag{16}$$

$$V = \frac{v}{V_{\text{pipe}}}, \tag{17}$$

$$T = \frac{T_f}{T_{\text{pipe}}}. \quad (18)$$

The initial conditions of the system are placed on the jets from where the air is discharged. They are written for the two components of the velocity, for the temperature, and for the turbulent energy: $U_0 = 1.4$, $V_0 = 0$, $T_0 = 1.22$, $k_0 = 0.0095$. The pressure drop between the upper and the lower parts of the pipe was not been taken into account, so the inlet velocities of each jet are the same.

The boundary conditions on the top of the system correspond to symmetry conditions, and they are defined as follows:

$$v = 0, \quad (19)$$

$$\frac{\partial u}{\partial r} = 0, \quad (20)$$

$$\frac{\partial T_f}{\partial r} = 0, \quad (21)$$

$$\frac{\partial k}{\partial r} = 0. \quad (22)$$

There are free flow conditions at the bottom of the system and some values, such as the outer part of the system, are defined there:

$$U = U_{\min} = 0.191 U_0, \quad (23)$$

$$\frac{\partial v}{\partial r} = 0, \quad (24)$$

$$T = T_{\text{out}} = 0.82 T_0, \quad (25)$$

$$k = k_{\text{out}} = 0.0526 k_0. \quad (26)$$

Due to the simplifications of the model, the equations that have to be solved are parabolic and it is necessary to set the outlet conditions.

2.3. Numerical procedure

Because of the symmetry of the system, as it was mentioned before, this problem was solved for the two-dimensional case taking into account only one slice of the total system. The discretization was done using the staggered grid with a finite difference scheme. The numerical algorithm used in order to solve the flow ejected by the jets through a particulate medium is the tri-diagonal matrix algorithm (TDMA), or the Thomas algorithm.

To include the effect of convection, the first-order upwind scheme was chosen because of its simplicity and stability. For turbulence modelling, the original formulation of the k–ε model with the addition of the particulate interactions was applied. The Boussinesq approach was used in order to include the effect of the temperature on the velocity of the flow.

3. RESULTS AND DISCUSSION

The calculations were made for different study cases in order to find how the variables evolve with changes in some parameters and how the parameters affect the whole system. The results are presented in plots using non-dimensional variables as it was explained above. The physical coordinates Y and X are also used in the non-dimensional form:

$$X = \frac{x}{R}, \quad (27)$$

$$Y = \frac{r}{R}. \quad (28)$$

3.1. Single-phase flow: effect of heating

In this first section, the calculations are made for the case of the single-phase flow, in order to obtain simple results and establish the bases for more complicated cases. The goal here is to understand how the result flow evolves, how the four jets interact and, finally, how the heating affects the velocity and turbulent kinetic energy fields. Two different cases are considered, one is isothermal, where the inlet flow has the same temperature as the system, and the other is the heated case, when the flows discharged by the jets have a higher temperature with the initial value explained above.

3.1.1. Effect on the axial gas velocity

The results show that the axial velocity starts with high values of each jet. Then, following the X direction the velocity peaks produced by each jet decrease, concentrate at the lowest values of Y and, finally, merge into one single jet (see Fig. 1).

Focusing on the values presented in Fig. 2, one can see that the flow merges quickly at the beginning. After that, the change of the velocity is slow as compared to the beginning. It is also important to notice that instead of expanding as a classical jet, the resulting flow contracts close to $Y = 0$. This effect takes place for all the variables calculated; this will be explained at the end of this section.

Figure 3 shows the difference between the isothermal case and the heated case in terms of the axial velocity in the slice $X = 19.9286$, which is the most representative.

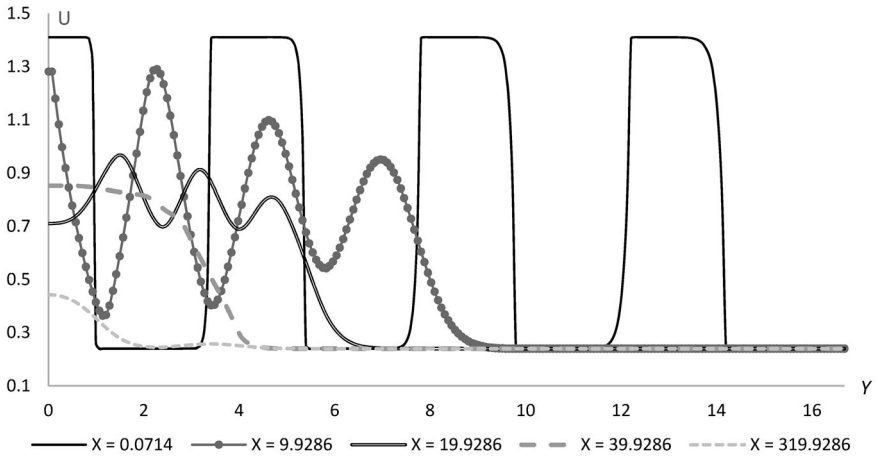

Fig. 2. Distribution and evolution of the axial gas velocity U for the isothermal case.

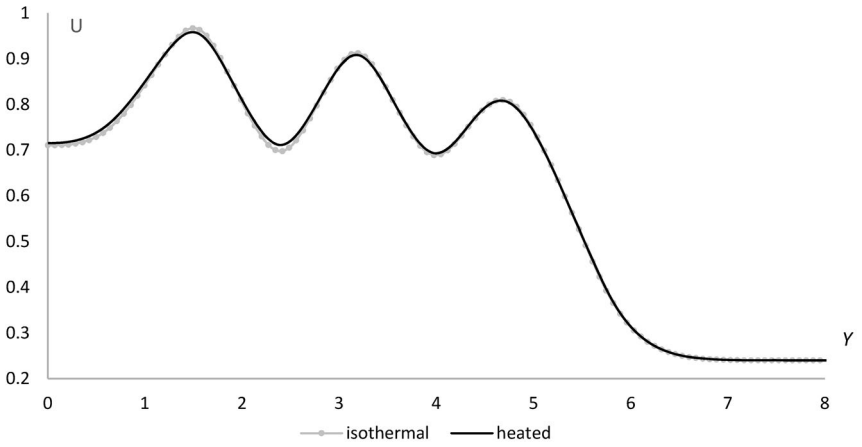

Fig. 3. Distribution of the axial gas velocity U at X = 19.9286 for the isothermal and heated cases.

The general shape of both cases is the same. The merging starts and the flow collapses at $Y = 0$, which is illustrated by the velocity peaks in Fig. 3. The difference in terms of values of the two cases is minimum. One can see that the isothermal case has a slightly higher amplitude of the peaks than the heated one, but essentially their behaviour is the same. This small effect is produced indirectly by the heating and the difference of densities that it produces, which will be explained in the part concerning the behaviour of the radial velocity.

3.1.2. Effect on the radial gas velocity

As one can see in Fig. 4, the jets induce radial velocity because of the drag caused by the ejection of airflow. Turbulence is also induced, seen as the variation of the velocity between positive and negative values. The radial velocity perturbations are dissipated quickly from $X = 0.0714$ to $X = 19.9286$.

Figure 5 shows the effect of heating on the radial gas velocity. This plot is the only one where the difference between the two cases is maximum. Heating produces an increase in the kinetic energy of the flow, as it is clearly seen in Fig. 5. The range of the radial velocity for the heated case is wider than for the isothermal case. As there is a huge decrease of the radial velocity in both cases and it changes from positive to negative values, one can say that the flow rotates faster for the heated case.

This effect is produced by the buoyancy forces acting on the fluid. As heating affects mostly the density of the fluid, the difference of densities produces a motion of the flow in the vertical direction; so heating affects the radial velocity directly and the U velocity indirectly. In addition, this effect has a small impact on the velo-

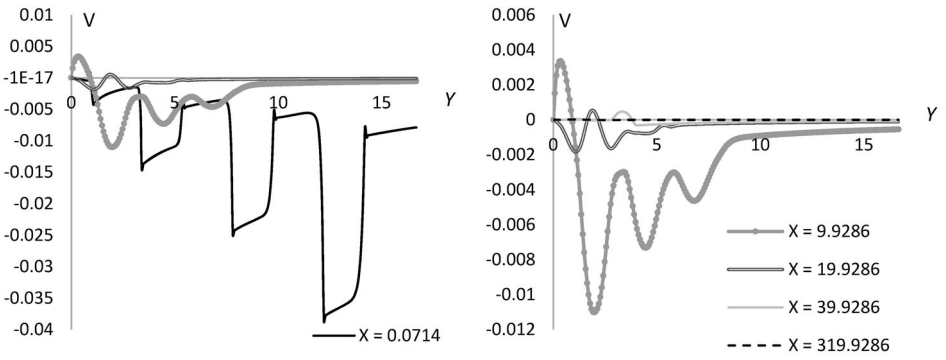

Fig. 4. Distribution and evolution of the radial gas velocity V for the heated case with (a) $X = 0.0714$ and (b) without it.

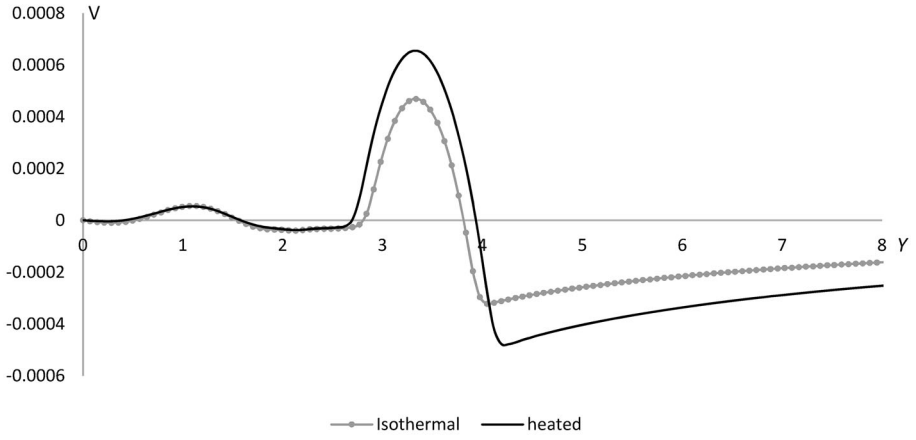

Fig. 5. Distribution of the radial gas velocity V at $X = 39.9286$ for the isothermal and heated cases.

cities of the system compared with the momentum of the jets [27].

3.1.3. Effect on the turbulent kinetic energy

The evolution of the turbulent kinetic energy has different stages (Fig. 6). First of all, the turbulence is generated by the jets, then, while the flow is merging, the turbulence also concentrates on the upper part of the system, showing high peaks of its kinetic energy. So, one can say that the second stage corresponds to the merging and increasing of turbulence. Following the X direction, the turbulence keeps merging, and the peak values decrease till the end of the jet sustem, where the flow is totally merged and the turbulence dissipates.

Figure 7 shows the difference between the isothermal and non-isothermal cases in terms of the turbulent kinetic energy at $X = 19.9286$. The shape of the field and the values for both cases are similar. The heated flow has lower values of the peaks close to the upper part of the system, but higher farther from it. It can be concluded that heating is conducive to merging because it makes the peaks tend to the same value, decreasing the amplitude of the high ones close to $Y = 0$ and increasing the small ones further.

3.2. Multi-phase flow: inclusion of particles

After the analysis of the single-phase flow, more complicated cases were calculated and analysed. Now particles were introduced into the system and the calculations were made for wood pellets ($\rho_p = 650$ kg/m^3) of 20 mm mean diameter at different particles volume fractions ($\beta = 0$, 0.002, and 0.02).

3.2.1. Effect on the axial gas velocity

The plots of the axial velocity demonstrate that the single-phase flow has a smaller amplitude of the peaks than the two-phase case (Fig. 8). Moving in the X direction,

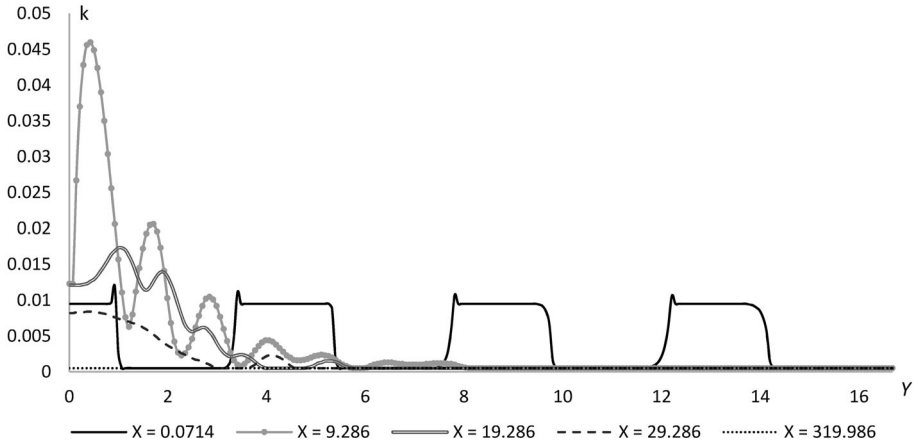

Fig. 6. Evolution of the turbulent kinetic energy k for the isothermal case.

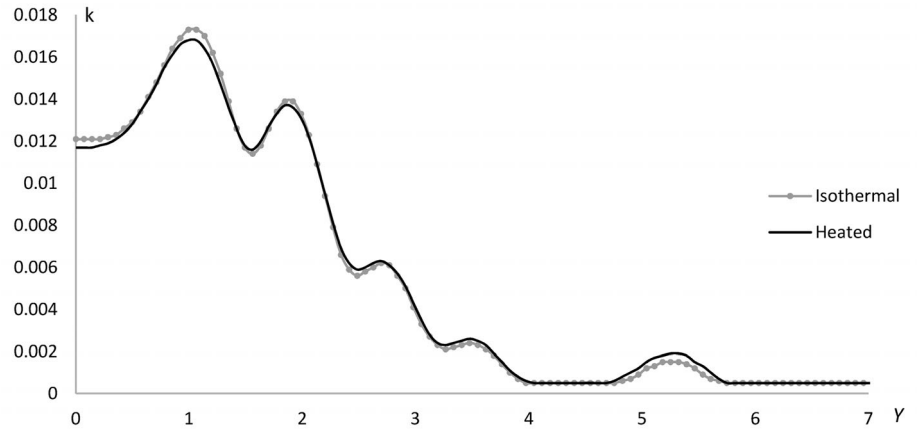

Fig. 7. Distribution of the turbulent kinetic energy k at $X = 19.9286$ for the isothermal and heated cases.

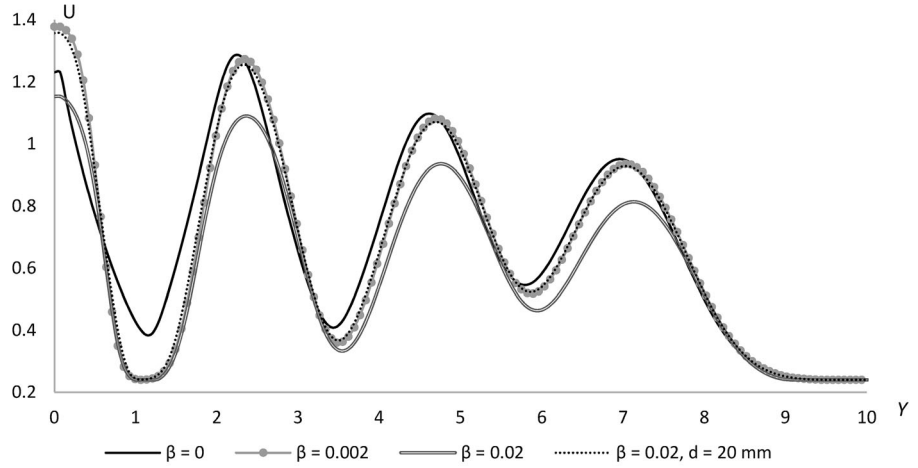

Fig. 8. Distribution of the axial gas velocity U at $X = 9.9286$ for different particles volume fractions.

it keeps the higher value until the flow totally merges (Fig. 9). In addition, the single-phase flow merges faster than the two-phase flow.

For the two-phase calculations, the increase of the particles volume fraction leads to an acceleration of merging (the velocity peaks are higher for the small volume fraction), and also a reduction of the maximum velocity when the jets merge. This is clearly shown in Fig. 9, where the case of the volume fraction of 0.02 has lower velocity than the one for 0.002. This effect occurs due to the increase of the drag produced by the increase of the volume fraction, which breaks the velocity and reduces the turbulent kinetic energy of gas.

To sum up, the single-phase flow shows a slower dissipation of velocity. For the two-phase flow, the dissipation is faster for the larger volume fraction of particles.

3.2.2. Effect on temperature

Focusing on the evolution of the temperature for the case of the volume fraction of 0.002 (Fig. 10), one can see that the inlet flow through the jets is hot and introduces thermal energy to the system. When increasing the X coordinate, the merging is clearly observed, the temperature in general dissipates due to the interaction with the particles, but the peaks are still visible, gathering into one single jet flow (cf. $X = 9.9286$ and $X = 39.9286$).

Figure 11 shows the difference between the single-phase case and some two-phase cases with different particle volume fractions and sizes. As can be observed, the merging is different for the single-phase and the two-phase flow. The former has regular peaks of temperature produced by the inlet condition, but the two-phase cases have some temperature peaks that merge.

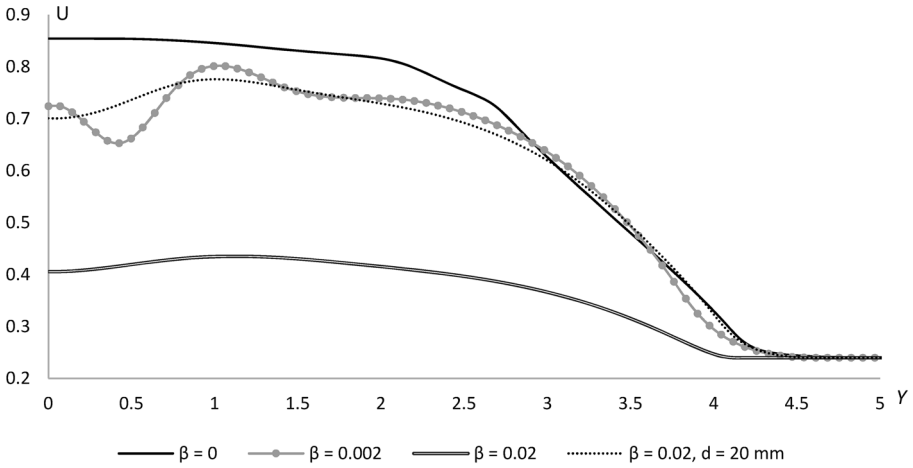

Fig. 9. Distributions of the axial gas velocity U at $X = 39.9286$ for different particles volume fractions.

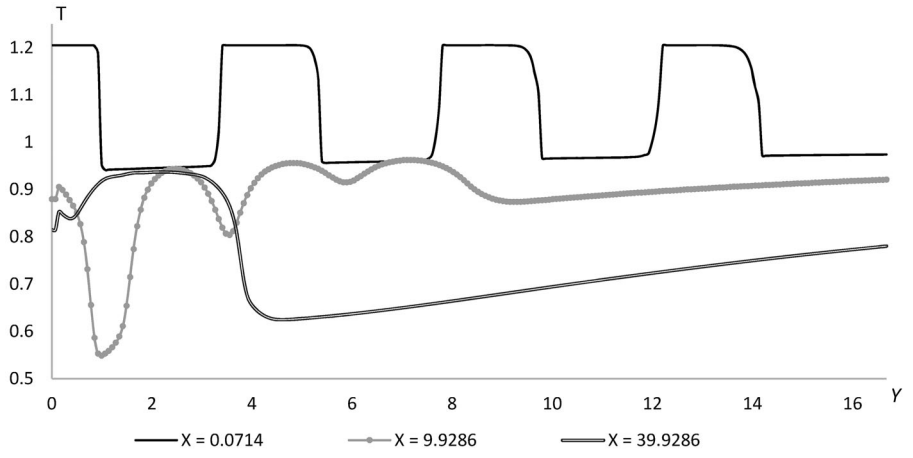

Fig. 10. Evolution of the temperature T for the case of particles volume fraction $\beta = 0.002$.

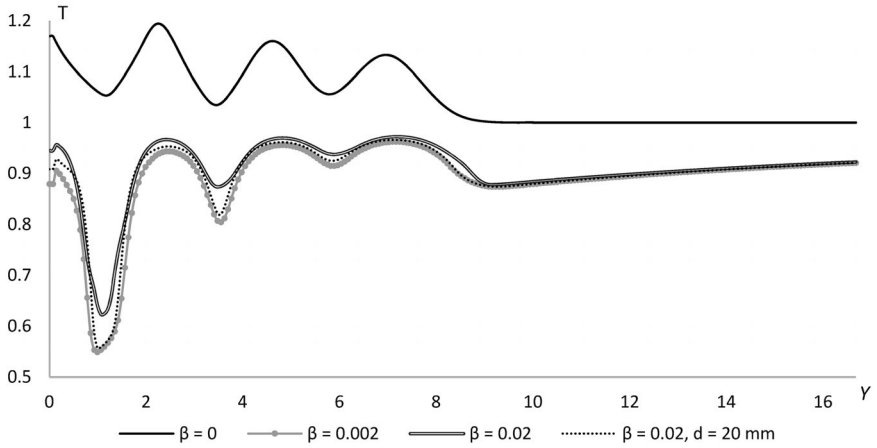

Fig. 11. Distributions of the temperature T at $X = 9.9286$ for different particles volume fractions β.

In addition, the dissipation of the temperature is higher for all two-phase cases because the single phase has no particles to exchange the energy.

Comparison of the two cases with different particle volume fractions indicates that the temperature dissipates more and merges less for the case of the smaller volume fraction.

3.2.3. Effect on the turbulent kinetic energy

In this section the results concerning the turbulent kinetic energy are presented and analysed for the flow through particulate media. The evolution of the turbulent energy in different slices of X for the case of 0.002 volume fraction and the particles diameter of 20 mm is illustrated in Fig. 12.

As it was explained in the single-phase section, turbulence is induced by the jets. However, in this case the three stages are different. The inclusion of particles changes the turbulence field. The turbulence induced by the jets starts to dissipate when the flow begins to merge, and so there is no increase of the values of turbulent kinetic energy close to $Y = 0$; the inclusion of particles dissipates turbulence faster than in the single-phase flow. It should also be noted that the contraction of the flow concentrates turbulence close to the upper part of the system, keeping the zero values of turbulence far from this section, where the flow barely affects the system.

Comparison of the cases of different particles volume fractions and sizes and the single-phase flow shows that the single-phase flow increases turbulence at the beginning of the merging (Fig. 13). This increase concentrates at the upper part of the system, and all the flows through particles reduce it.

Focusing on the effect of different volume fractions of 20 mm particles, Fig. 13 shows that turbulence dissipates faster for smaller particles volume fractions.

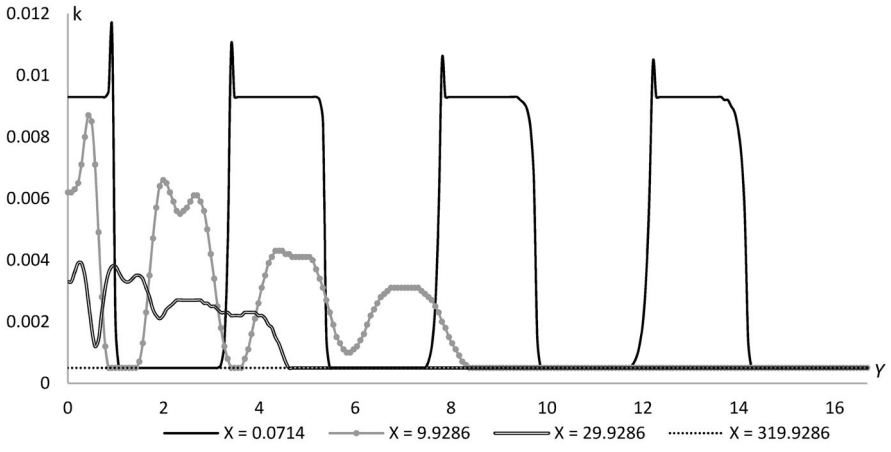

Fig. 12. Evolution of the turbulent kinetic energy k for the case of particles volume fraction $\beta = 0.002$.

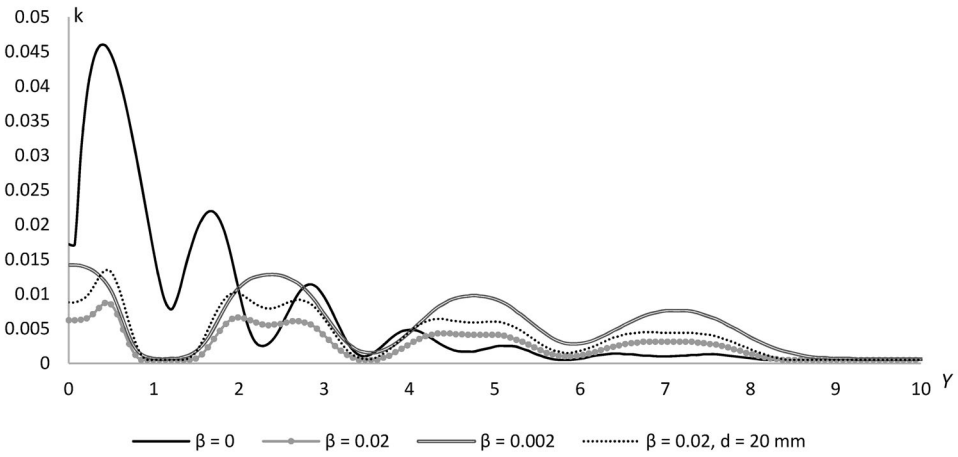

Fig. 13. Distribution of the turbulent kinetic energy k at $X = 9.9286$ for different particles volume fractions β.

3.3. General remarks

Having studied all the different cases and analysed the effects of heating and variation of the volume fraction, some reflections can be provided.

Taking a look at the general behaviour of all the cases, without focusing on the specific modifications produced by the variations of the parameters, one can see that the jets merge into a single jet with the disappearance of the velocity peaks produced by the jets and concentrate in the upper part of the system within a relatively short distance of up to $X = 39.9286R$, against the total distance of $319.9286R$. This effect occurs for all the cases: isothermal, heated, and with the inclusion of particles. Such behaviour is explained in different studies of the twin jets and their interactions [28]. It is experimentally determined that by increasing the Reynolds number or decreasing the spacing between the jets, the turbulent energy and interference increase and the twin jets attract strongly due to the suction produced by the surface and the adjacent flows. For the system of two jets, at first a clear separation of the twin jets near the nozzle takes place, then interaction of the two jets occurs, and, finally, the jets mix and merge into a single jet [28]. This perfectly explains what happens in our system. As the separation between jets decreases, they collapse while merging instead of expanding, which results in a single jet flow.

All the calculations follow this behaviour of collapsing instead of expanding. The modification of the parameters, such as heating and the particles volume fraction, only changes the values of the velocities, temperature, or kinetic turbulent energy, increasing or decreasing the dissipation and accelerating or breaking the merge.

4. CONCLUSIONS

- The multiple jet system discharging from a turbulent non-isothermal air flow is a very complicated case of fluid dynamics. This study shows that the jets interact with each other as well as with the boundaries, making them difficult to calculate. In addition, if particles are included, it becomes a two-phase problem with more interactions. The four jets merge and collapse near $Y = 0$ due to the small separation between them.
- For a single-phase flow, the four jet flows merge into a single jet, located at the top of the system. The turbulent kinetic energy increases during merging before dissipation starts. Heating mainly affects the velocity, through the buoyancy effect, directly increasing the radial gas velocity and indirectly affecting the axial gas velocity.
- The inclusion of particles generally produces a slower merging than for the single-phase case, increases the dissipation of temperature, and dissipates the turbulent energy since the merging starts. Concerning only the calculations with particles, increasing the particles volume fraction accelerates the merging and the dissipation of velocity and decreases the dissipation of temperature and turbulence.
- The further steps of this study should take into account the pressure drop between the top and the bottom, before the inlets, to make the model more realistic with different inlet velocities of each jet. In addition, to see how the merging and the evolution of the flow take place, the parameter that should be varied is the distance between the jets. Another important parameter that should be considered is the relative humidity of the particles.

ACKNOWLEDGEMENTS

The authors are grateful to Texas Advanced Computing Center (TACC) in Austin, USA, for the technical support. Support from the Estonia–Norway project EMP230 is gratefully acknowledged. This study is related to the activity of the European network action COST MP1106 'Smart and green interfaces – from single bubbles and drops to industrial, environmental and biomedical applications'.

The publication costs of this article were covered by the Estonian Academy of Sciences.

REFERENCES

1. Noyes, R. T. Development of a new low-energy environmentally compatible grain and seed drying storage technology. In *Proceedings of the 9th International Working Conference on Stored Product Protection, São Paulo*. 2006, 1285–1294.
2. Day, D. and Nelson, G. *Predicting Performances of Cross-flow Systems for Drying Grain in Storage in Deep Cylindrical Bins.* ASAE Paper No. 62-925. American Society of Agricultural Engineers, St. Joseph, Mich., USA, 1962.
3. Navarro, S., Noyes, R., and Armitage, D. *Supplemental aeration systems. The Mechanics and Physics of Modern Grain Aeration Management*. CRC Press, Boca Raton, 2002, 417–424.
4. Jayas, D. and Muir, W. Air flow pressure drop data for modelling fluid flow in anisotropic bulks. *Transactions of the ASAE*, 1991, **34**(1), 251–254.
5. Jayas, D. and Mann, D. Presentation of airflow resistance data of seed bulks. *Appl. Eng. Agric.*, 1994, **10**(1), 79–83.
6. Narasimhan, A. *Essentials of Heat and Fluid Flow in Porous Media*. CRC Press, Taylor and Francis Group, India, 2012.
7. Ljung, A., Lundström, T. S., and Tano, K. Simulation of heat transfer and fluid flow in a porous bed of iron ore pellets during up-draught drying. In *Proceedings of the 5th International Conference on CFD in the Process Industries, Melbourne 2006*. http://www.cfd.com.au/cfd_conf06/PDFs/108Lju.pdf (accessed 2015-11-09).
8. Mitkov, I., Tartakovsky, D. M., and Winter, L. Dynamics of wetting fronts in porous media. *Phys. Rev. E. J.*, 1998, **58**, 5245–5248.
9. Abramovich, G. Effect of admixture of solid particles or droplets on the structure of a turbulent gas jet. *Int. J. Heat Mass Flow*, 1971, **14**, 1039–1045.
10. Gore, R. and Crowe, C. Effect of particle size on modulating turbulent intensity. *Int. J. Multiphase Flow*, 1989, **15**, 279–285.
11. Yuan, Z. and Michaelides, E. Turbulence modulation in particulate flows, a theoretical approach. *Int. J. Multiphase Flow*, 1992, **18**, 779–785.
12. Hetsroni, G. and Sokolov, M. Distribution of mass, velocity and intensity of turbulence in a two-phase turbulent jet. *Trans. ASME J. Appl. Mech*., 1971, **38**, 315–327.
13. Laats, M. and Frishman, F. Development of the method and research of turbulence intensity at two-phase jet axis. *Izv. AN USSR*, 1973, **2**, 153–157 (in Russian).
14. Shraiber, A. A., Yatsenko, V. P., Gavin, L. B., and Naumov, V. A. *Turbulent Flows in Gas Suspensions*. Hemisphere, New York, 1990.
15. Frishman, F., Hussainov, M., Kartushinsky, A., and Mulgi, A. Numerical simulation of two-phase turbulent pipe-jet flow loaded polydispersed solid admixture. *Int. J. Multiphase Flow*, 1997, **23**, 765–796.
16. Almeida, T. and Jaberi, F. Large-eddy simulation of a dispersed particle-laden turbulent round jet. *Int. J. Heat Mass Transfer*, 2008, **51**, 683–695.
17. Kartushinsky, A., Michaelides, E., Rudi, Y., and Nathan, G. RANS modelling of a particulate turbulent round jet. *J. Chem. Eng. Sci.*, 2010, **65**, 3384–3393.
18. Crowe, C. T. and Gillandt, I. Turbulence modulation of fluid–particle flows, basic approach. In *Proceedings of the 3rd Int. Conference on Multiphase Flows, Lyon, 1998*. CDROM.
19. Zaichik, L. and Alipchenkov, V. Statistical models for predicting particle dispersion and preferential concentration in turbulent flows. *Int. J. Heat Fluid Flow*, 2005, **26**, 416–430.
20. Corrsin, S. Investigation of the behaviour of parallel, two-dimensional air jets. *NACA*, 1944, No. 4H24.
21. Marsters, G. Measurements in the flow field of a linear array of rectangular nozzles. *J. Aircraft*, 1979, **17**, 774–780.
22. Yimer, I., Becker, H., and Grandmaison, E. Development of flow from multiple-jet burners. *Can. J. Chem. Eng*., 1996, **74**, 840–851.
23. Böhm, B., Stein, O., Kempf, A., and Dreizler, A. In-nozzle measurements of a turbulent opposed jet using PIV. *Flow Turbul. Combust.*, 2010, **85**, 73–93.
24. Rieth, M., Proch, F., Stein, O., Pettit, M., and Kempf, A. Comparison of the sigma and Smagorinsky LES models for grid generated turbulence and a channel flow. *J. Computers & Fluids*, 2014, **99**, 172–181.
25. Schiller, L. and Naumann, A. Über die grundlegenden Berechnungen bei der Schwerkraftaufbereitung. *Z. Vereines Deutscher Ingenieure*, 1933, **77**, 318–320.
26. Abramovich, G. 1963. *The Theory of Turbulent Jets*. The MIT Press Classics, Boston, 1963.
27. Ihme, M. and Pitsch, H. Effects of heat release on turbulent jet flows. In *Proceedings of the 5th International Symposium on Turbulence and Shear Flow Phenomena, Munich*. 2007.
28. Zhao-qin Yin, Hong-jun Zhang, and Jian-Zhong Lin. Experimental study on the flow field characteristics in the mixing region of twin jets. *J. Hydrodyn.*, 2007, **19**, 309–313.

*Proceedings of the Estonian Academy of Sciences, 2016, **65**, 3, 195–204*

Turbulentsete jugavooluste kogumi liikumine läbi osakestega täidetud staatilise keskkonna

Peep Lauk, Josep Hueso Rebassa, Aleksander Kartushinsky, Sergei Tisler, Toivo Tähemaa ja Andrei Polonsky

Töö koosneb kahefaasilise vooluse numbrilisest modelleerimisest poorse keskkonna tingimustes. Pelletikuivataja tööd modelleeritakse voolamisena vertikaalses silindris, millel on neli külgdüüsi õhu sisselaskmiseks kuivatatavate osakeste liikumatusse keskkonda. Käesoleva töö eesmärk on paremini tunnetada soojusvahetuse mehhanismi ja seda, kuidas erinevad parameetrid mõjutavad keskkonda läbivat gaasi, et konstrueerida optimaalset kuivatit. Voolust käsitletakse mitteisotermilisena ja arvestatakse niiskusesisalduse muutumisega lõplike vahede skeemi. Läbiarvutatud juhtumid on esiteks ühe faasi jaoks (isotermiline ja mitteisotermiline) ning siis kahe faasi jaoks, muutes osakeste mahuosa ja nende suurust. Selleks et arvesse võtta temperatuuri mõju gaasi kiirusele, kasutati Boussinesqi lähendust ja momendivõrrandite sulgemiseks rakendati k–ε mudelit. Tulemused näitavad erinevate muutujate – eelkõige telg-kiiruse ja külgjugade temperatuuri – mõju väärtustele. Sisselaske juures olevad kõrged väärtused vähenevad voolu keskkonna läbimisega. Muutus on suurem osakeste suurema mahu korral, sest see takistab voolu. Radiaalne kiirus kaldub suurenema nullist kiiremini suurema osakeste mahuosa korral, kuna need muudavad voolu suunda. Temperatuur langeb kiiremini suurema osakeste mahuosa korral ja suuremate osakeste puhul, sest takistusjõud suureneb, mida saab tõlgendada kui suurenenud energiaülekannet vooluse ning osakeste vahel.